

Phase-Locked Two-Dimensional Array of Vertical Cavity Surface Emitting Lasers

Hoi-Jun Yoo, J. R. Hayes, E. G. Paek, J. P. Harbison, L. T. Florez, and Young-Se Kwon*

BELLCORE, 331 Newman Springs Road, Red Bank, NJ 07701-7040, USA.

*Dept. of E.E., KAIST, Cheongryang P.O. Box 150, Seoul, Korea.

We report the characteristics of two-dimensional phase-locked arrays of vertical cavity surface emitting lasers. Three different two-dimensional array structures have been realized, they are a 2 x 3 periodic array of 10 μ m squares, a hexagonal array and a centered hexagonal array of 5 μ m hexagons. All arrays were fabricated using the same technique which was a combination of mesa etching and oxygen implantation isolation. The threshold current of 2 x 3 periodic array was 24mA, hexagonal array was 30mA and centered hexagonal array was 22mA. The far field beam angle was about 2 $^\circ$. The centered hexagonal array has the most circularly symmetric far field beam pattern.

I. Introduction

Recently, there has been intense interest in two-dimensional arrays of surface emitting lasers for a variety of applications requiring high output power, narrow far-field beam divergence and high energy conversion efficiency.[1-4] Two-dimensional arrays of laser diodes have many advantages over the linear arrays. Some of the advantages are a higher power capability coming from the wide active area, improved directionality resulting from the large emitting area of the source and greater flexibility in the geometry of array structures that allows the output beam to be tailored.

Since the vertical cavity surface emitting laser diode (VC-SEL) can be fabricated using a fully monolithic process, it is easy to integrate these structures into closely packed two dimensional arrays for realizing phase locked arrays. Also, the performance of VC-SEL's has improved significantly over the last year such that a low threshold, high quantum efficiency and high power operation can be obtained.[5-6]

In a previous paper[7], we proposed and categorised two-dimensional arrays into 3 basic

structures, the periodic array, the circular array and the concentric circular array, following the convention in microwave antenna theory. In that paper, the near-field and far-field patterns of each array structure had been analyzed and compared. In this paper, we report the experimental realization of monolithic two-dimensional phased arrays of VC-SEL's.

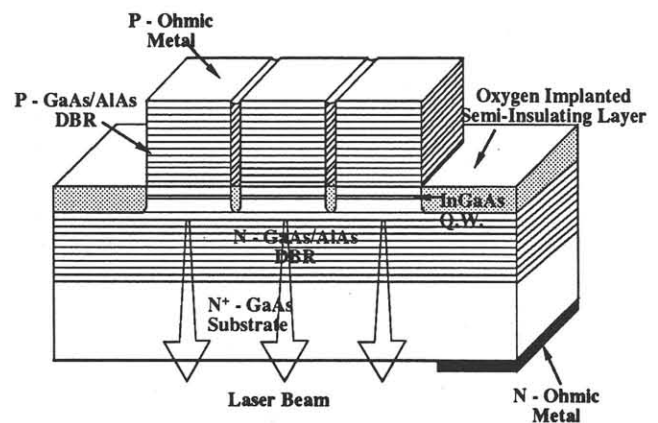


Fig.1 Schematic diagram of mesa etched-implant isolation array structures.

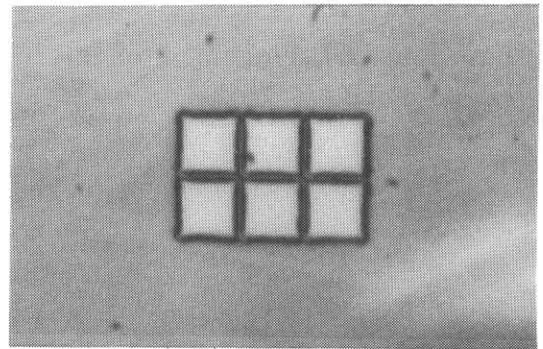
II. Fabrication

The two-dimensional arrays were fabricated using implant-isolated mesa etched VC-SEL's. A schematic crosssectional diagram of the array structure is shown in Fig. 1. The lasers consisted of an undoped 100Å strained $\text{In}_{0.2}\text{Ga}_{0.8}\text{As}$ active region clad by an $\text{Al}_{0.5}\text{Ga}_{0.5}\text{As}$ cavity layer of an optical wavelength thickness and distributed Bragg reflector (DBR) mirrors consisting of 20 periods of AlAs/GaAs grown on a n^+ -GaAs substrate by molecular beam epitaxy. The bottom mirror was doped n-type with Si to $3 \times 10^{18} \text{cm}^{-3}$ and the top mirror was doped p-type with Be to $5 \times 10^{18} \text{cm}^{-3}$. The structure was completed with the growth of a thin p^+ contact layer.

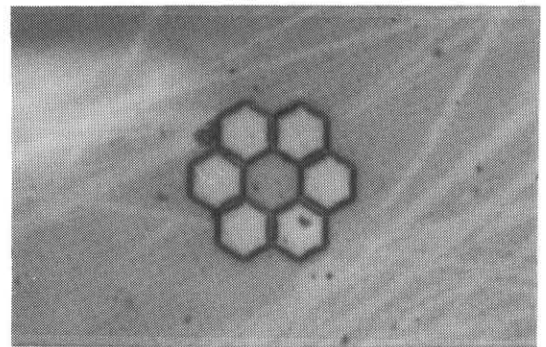
After the growth, a thick photoresist layer, $\sim 3 \mu\text{m}$, was coated and patterned into the various array structures, the periodic, circular and concentric circular arrays. This photoresist mask served as the etch mask for ion beam milling through the p-DBR to a point near the upper AlGaAs cavity layer, $\sim 0.2 \mu\text{m}$ above the cavity layer. After the etching, a double oxygen ion beam implant was performed at 300KeV and 80KeV with a dose of 1×10^{15} to electrically isolate each device. The same photoresist was used as the implant mask. The implanted semi-insulating region penetrates the active region down to the top of the n-type DBR to isolate each elemental laser.

The processing continued with the application of a thick planarizing layer of polyimide. The polyimide was then etched using an oxygen plasma until the individual laser of the array were exposed. The structure was then coated with a 2500Å thick gold layer. The other side of substrate was polished with $\text{Br}_2\text{-MeOH}$ solution and bonded on the glass plate using indium solder. A small probe tip was then placed on the p-contact and the output beam of the array was monitored through the substrate and glass plate.

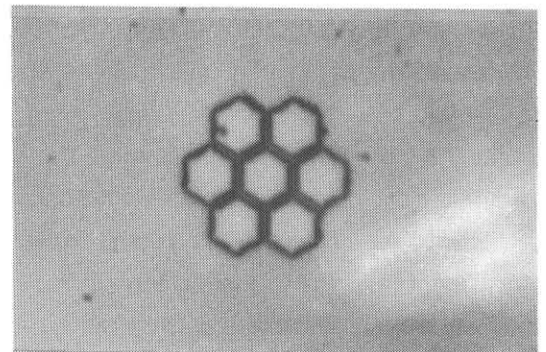
Microphotographs of the fabricated two-dimensional arrays are shown in Fig.2. Fig. 2(a) shows a 2x3 periodic array of $10 \mu\text{m}$ square



2x3 Periodic Array



Hexagonal Array



Centered Hexagonal Array

Fig.2 Microphotographs of (a) a 2 x 3 periodic array, (b) a hexagonal array and (c) a centered hexagonal array.

VC-SEL and a hexagonal array (a circular array) of $5 \mu\text{m}$ hexagonal lasers is shown in Fig. 2(b). Fig. 2(c) is a microphotograph of a centered hexagonal array (a concentric circular array) also comprised of $5 \mu\text{m}$ hexagonal lasers. The separation between each VC-SEL is $1 \mu\text{m}$ and all VC-SEL's are pumped jointly.

III. Experimental Results

The light output / current characteristics of each array was measured under 200ns pulse at repetition rate of 500kHz and is shown in Fig. 3. The hexagonal array had the highest threshold current of 30mA, the centered hexagonal array had 22mA and the 2 x 3 periodic array had 24mA. The area of the array aperture size of 2 x 3 periodic array is wider than that of hexagonal array leading to higher threshold current but larger maximum power output. Although the hexagonal array has a less area than centered hexagonal array, it shows higher threshold current. This results from the small overlap of the optical field among element lasers. In the centered hexagonal array, the center laser can increase the coupling among the elemental lasers by sharing of the optical gain to reduce the threshold current.

The near field patterns of the fabricated arrays above the lasing threshold are shown in Fig. 4. The intensity of each laser is not uniform due to growth nonuniformity. This effect determines the initial far field pattern. However, it approaches a symmetric

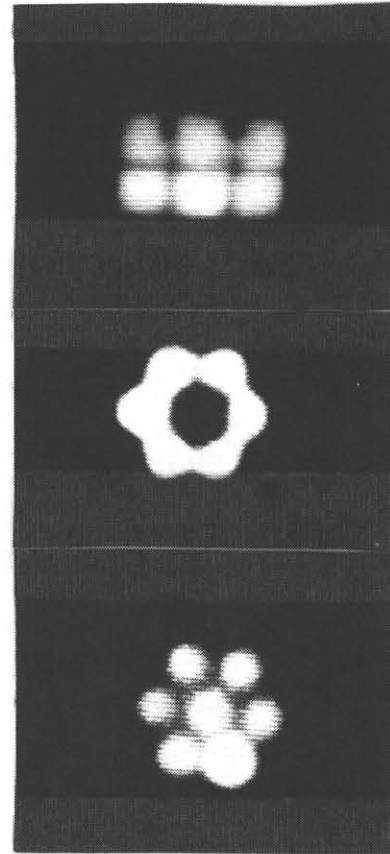


Fig.4 Microphotographs of the near field patterns of (a) a 2 x 3 periodic array, (b) a hexagonal array and (c) a centered hexagonal array.

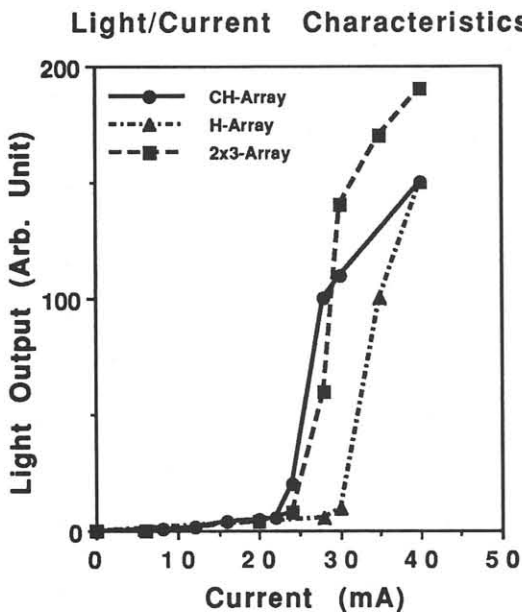


Fig.3 Light output vs. current characteristics of fabricated two-dimensional phased arrays.

pattern as the injection current increases. Fig. 5 shows an example of the mode change with the injection current level. We believe the mode competition is initially governed by the local gain. However with an increase in the injection current the mode is determined by the global gain which is dictated by the symmetry of the structure.

Fig. 6 shows the far-field patterns of the fabricated arrays. Centered hexagonal array shows the most circularly symmetric beam pattern. The beam width is 2° which is a clear evidence of the phase-locking of the individual lasers. The 2 x 3 periodic array had a two-lobed beam pattern where the separation of the lobes was 1.5° . The hexagonal array had concentric circles but its center had a null

of optical power. The array mode for this far field pattern can be predicted to have the same distribution of the 1st mode of benzene molecular orbital.

IV. Conclusions

In conclusion, we fabricated three different array structures, a 2 x 3 periodic array of 10 μ m square lasers, a hexagonal array and a centered hexagonal array of 5 μ m hexagonally structured lasers. The centered hexagonal array has the lowest threshold current because it has a largest optical coupling between elemental lasers. The near field patterns of the arrays depends on the laser uniformity and the global symmetry of the array structures. The centered hexagonal array has the most circularly symmetric far field beam pattern and 2 x 3 array has the least circularly symmetric far field beam. The narrow far field beam angle of 2 $^{\circ}$ shows clear evidence that phase-locking of the individual lasers has occurred.

Reference

1. G.A. Evans et al., Appl. Phys. Lett., vol. 53, pp.2123-2125, Nov. 1988.
2. J.J. Yang et al., Fiber and Integrated Optics, vol.7, pp.217-228, 1988.
3. Z. L. Liao and J.N. Walpole, Topical Meeting on Semiconductor Lasers, Feb. 1987, paper WA2, pp.84-86.
4. Hoi-Jun Yoo et al., Appl. Phys. Lett., Vol. 56, pp.1198-1200, 1990.

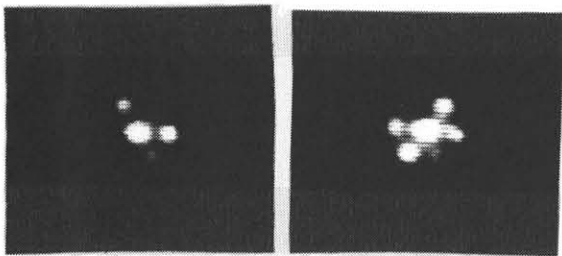


Fig.5 Current dependence of the near field pattern of the centered hexagonal array. (a) At low injection level, pattern was dictated by the local gain. (b) With the increase of the current, it approached a symmetric pattern.

5. K. Iga et al., IEEE J. Quantum Electron. , vol. 24, pp.1845-1855, Sep. 1988.
6. J. L. Jewell et al., Electron. Lett., vol.25, pp.1123-1124, 1989.
7. Hoi-Jun Yoo et al., IEEE J. Quantum Electron., June (1990).



Fig.6 Far field beam patterns of (a) a 2 x 3 periodic array, (b) a hexagonal array and (c) a centered hexagonal array.